



Slow and steady wins the race: physical limits on the rate of viral DNA packaging

Paul J Jardine

During the assembly of dsDNA viruses such as the tailed bacteriophages and herpesviruses, the viral chromosome is compacted to near crystalline density inside a preformed head shell. DNA translocation is driven by powerful ring ATPase motors that couple ATP binding, hydrolysis, and release to force generation and movement. Studies of the motor of the bacteriophage phi29 have revealed a complex mechanochemistry behind this process that slows as the head fills. Recent studies of the physical behavior of packaging DNA suggest that surprisingly long-time scales of relaxation of DNA inside the head and jamming phenomena during packaging create the physical need for regulation of the rate of packaging. Studies of DNA packaging in viral systems have, therefore, revealed fundamental insight into the complex behavior of DNA and the need for biological systems to accommodate these physical constraints.

Address

Department of Diagnostic and Biological Sciences, University of Minnesota, 18-242 Moos Tower, 515 Delaware St SE, Minneapolis, MN 55455, United States

Corresponding author: Jardine, Paul J (jardine@umn.edu)

Current Opinion in Virology 2019, 36:xx-yy

This review comes from a themed issue on **Virus structure and expression**

Edited by **Juliana Cortines** and **Peter Prevelige**

<https://doi.org/10.1016/j.coviro.2019.03.002>

1879-6257/© 2018 Elsevier Ltd. All rights reserved.

Learning from living systems

Given that biological systems have adapted to the constraints of the physical world for a billion years, the study of biology serves to inform us as to how things work. The cross-section of the bird wing reveals the principles of aerodynamic lift. The surface of the *Nelumbo* leaf demonstrates the principles of superhydrophobicity. And the behavior of DNA in viruses reveals the complexities of how charged polymers interact.

For viruses, the key biological challenge is to deliver their parasitic genome from one host cell to the other. The study of virus assembly focuses on the events that yield a

vehicle capable of accomplishing this task, with the double-stranded DNA viruses adopting a build-and-fill strategy whereby the protein capsid is constructed and then filled with genetic cargo [1[•]]. The challenge this presents is formidable, given that most dsDNA viruses compact their DNA chromosome to near crystalline density inside the capsid [2].

The utility of DNA as an information bearing molecule is confounded by the complex physical behavior its structure yields. On the scale of viruses, it is stiff, having a persistence length longer than the radius of the virus capsid [3]. Its phosphate backbone resists compaction due to charge repulsion [4]. And confinement inside a capsid comes with an entropic penalty as it is driven into a space that is orders of magnitude smaller than it would otherwise occupy. Therefore, in order to assemble a DNA-filled capsid the dsDNA viruses have evolved a machine capable of overcoming these resistive forces in order to package their DNA.

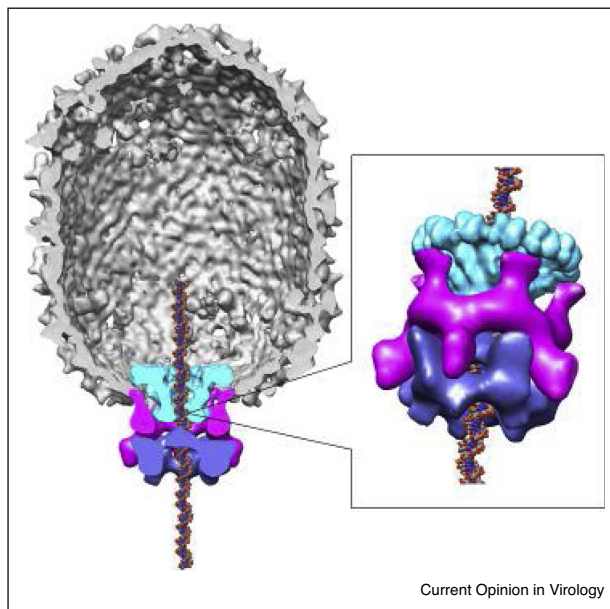
At first blush the challenge is one that can simply be overcome by brute force. The DNA packaging machines that translocate DNA, powered by ATP, have been shown to be among the most powerful measured [5]. One of the best characterized is the DNA packaging motor of the *Bacillus subtilis* bacteriophage phi29 [6], whose ring-motor gene product 16 (gp16) is of the ancient and diverse ASCE lineage that drive polymers across the biological continuum [7]. The gp16 pentamer forms the catalytic core of the packaging motor in phi29 [8], and is anchored to a fivefold vertex of the icosahedral capsid by an RNA scaffold [9,10], forming a ribonucleoprotein complex that will be discarded after packaging the DNA through a portal assemblage embedded in the capsid (Figure 1). The RNA scaffold, or pRNA, is unique to phi29, as most tailed dsDNA phages and the analogous herpesviruses employ only a portal and an ATPase [1[•]] (referred to as terminase in these systems; see below). Single-molecule studies have revealed that the phi29 motor can pull DNA with a measured force of over 57pN [11[•]], strong enough to begin to unwind the DNA helix if the DNA is tethered. But as with many things in biology, DNA packaging has revealed subtleties about the physical world that go beyond what were predicted or thought to be the limits of behavior.

Virus DNA packaging

The first measurements of the physical parameters of DNA packaging for a viral system were achieved using

2 Virus structure and expression

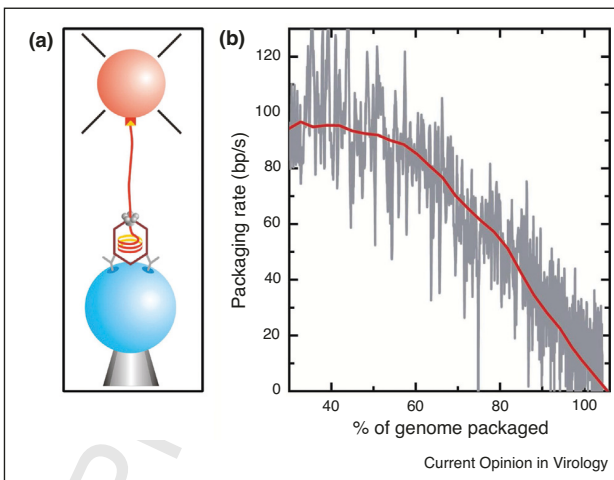
Figure 1



Current Opinion in Virology

Architecture of the phi29 DNA packaging motor. The pentameric packaging ATPase, gp16, (blue) is anchored to the capsid through the pentameric prohead RNA (pRNA) scaffold (magenta) and pushes DNA through the dodecameric connector portal (green). Reprinted from Mao *et al.* [8] with permission from Elsevier.

Figure 2



Early single-molecule measurements of phi29 DNA packaging using laser tweezers. (a) Packaging complexes were tethered between two microspheres, with the prohead/motor complex attached to one bead (blue) by antibodies against the capsid protein and the free end of the DNA attached to a second bead (orange) via a biotin-streptavidin linkage. (b) The change of tether length over time was used to calculate the change in packaging velocity over the course of head filling (grey trace is raw data; red trace is decimated and filtered). Reprinted from Chemla *et al.* [13] with permission from Elsevier (a) and Smith *et al.* [11*] with permission from Springer Nature (b).

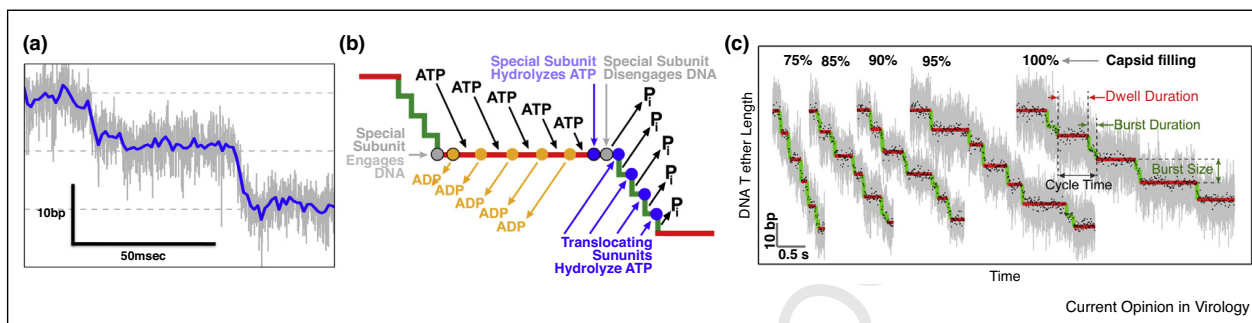
Q1

single-molecule laser tweezers on the phi29 system by Smith *et al.* in 2001 [11*]. Adapted from a robust bulk *in vitro* assay, phi29 DNA translocation was observed to be highly processive and dynamic (Figure 2). The first half of the full 19.6 kilobase complement of DNA moves at a rate of \sim 120 bp/s into the head shell. Thereafter the rate of packaging decreases noticeably, with the final segment moving at a snail's pace of \sim 10 bp/s (Figure 2b). The immediate inference was that this reduction in velocity was due to the motor encountering the resistive forces that are the result of DNA confinement. By emulating the response of the motor to increased load by pulling externally on the DNA in the laser tweezers, Smith *et al.* calculated a resistive force curve relative to DNA filling, and estimated that a force of 80 pN was required to drive the last of the DNA into the phi29 capsid. The magnitude of this force was unexpected, given that existing estimates of resistive force, derived from theoretical models that considered the stiff and self-repulsive nature of DNA, predicted a resistive force fivefold lower [12*]. As a result of these early experiments, a flurry of theoretical models emerged to either validate or challenge these force calculations.

Nearly two decades later, a more complex picture of phi29 DNA packaging has emerged that sheds light on some of the assumptions made while interpreting the

phenomena of reduced translocation velocity during head filling. Advanced, higher-resolution laser tweezers experiments in the Bustamante lab by Chemla, Moffit, Liu, and Chistol revealed the complex mechanochemistry of the phi29 packaging motor (Figure 3). Much of the time the motor does not move the DNA, but rather holds the DNA static while the ATPase subunits exchange waste ADP for new ATP [13–15]. These protracted 'dwells' take an average 125 ms during early stages of filling when resistive forces are at their lowest, and end with a relatively rapid translocating 'burst' where 10 bp of DNA moves into the head in 10 ms (hence the 'real' rate of translocation is closer to 1000 bp/s). Given that much of the overall velocity of DNA packaging is dominated by the non-mechanical dwell, the change in the actual speed of DNA entry over the course of head filling was reassessed [16**]. At the highest filling conditions assayed, it was found that the burst duration increased to \sim 80 ms. Again, the internal resistive force was estimated by comparing the reduction in DNA movement velocity in response to external tensioning force, this time yielding a calculation of \sim 20 pN. This value is much closer to that originally predicted by theory [12*], thus reconciling the issue to this point. But whereas one discrepancy was addressed in the field, a new and more puzzling one emerged: what causes the composite speed of packaging to decrease so dramatically during head filling?

Figure 3



Mechanochemistry of the phi29 DNA packaging motor. (a) Plot of DNA tether length versus time showing the dwell-burst cycle of DNA packaging using high-resolution single-molecule laser tweezers (grey trace is raw data; blue trace is decimated and filtered). (b) The corresponding mechanochemical scheme showing the order and timing of the ATPase cycle within the motor ring and DNA movement, where ADP is exchanged for ATP during the static dwell (red line) and mechanical stepping (consisting of four 2.5 bp substeps) occurs during the burst (green line). (c) Changes in dwell and burst duration over the course of head filling. As the head fills, much of the reduction in DNA translocation rate is due to the lengthening of the static dwell (red lines) rather than the dynamic burst (green lines). Reprinted from Liu et al. [16*] with permission from Elsevier.

140 The answer, in part, resides in the enzymatic behavior of
 141 the ATPase ring [15,16*]. During low filling, when
 142 resistive forces are believed to negligible, the motor is
 143 able to cycle nucleotide substrate quickly, with a calcu-
 144 lated V_{max} of 120 bp/s and a K_m of 30 μ M. As the head
 145 approaches becoming full, the V_{max} drops to 10 bp/sec
 146 and the K_m to 10 μ M. Thus, the ratio of V_{max}/K_m goes
 147 from 4 to 1 bp/s/ μ M, in large part due to a reduction in
 148 ATP tight binding rate, which is the last step before
 149 entering the burst. It has been proposed that this is due to
 150 an allosteric signal from inside the head, possibly by or
 151 through the connector-portal complex, that reduces the
 152 nucleotide cycling efficiency of the ATPase. However, a
 153 more confounding question emerges: why does the motor
 154 slow down when it has ample force-generating capacity to
 155 continue moving DNA at a faster rate?

156 Insight into DNA behavior

157 Over the past five years, evidence has emerged from
 158 parallel studies into the behavior of DNA under confine-
 159 ment in the phi29 capsid that sheds light on this question.
 160 In studies conceived to determine the effects of charge
 161 screening on the resistive force opposing packaging and
 162 whether energy dissipates from the packaged DNA over
 163 time, Berndsen and Keller in the Smith lab began a series
 164 of experiments that reveal phenomena that provide
 165 insight into the slowing of the packaging motor.

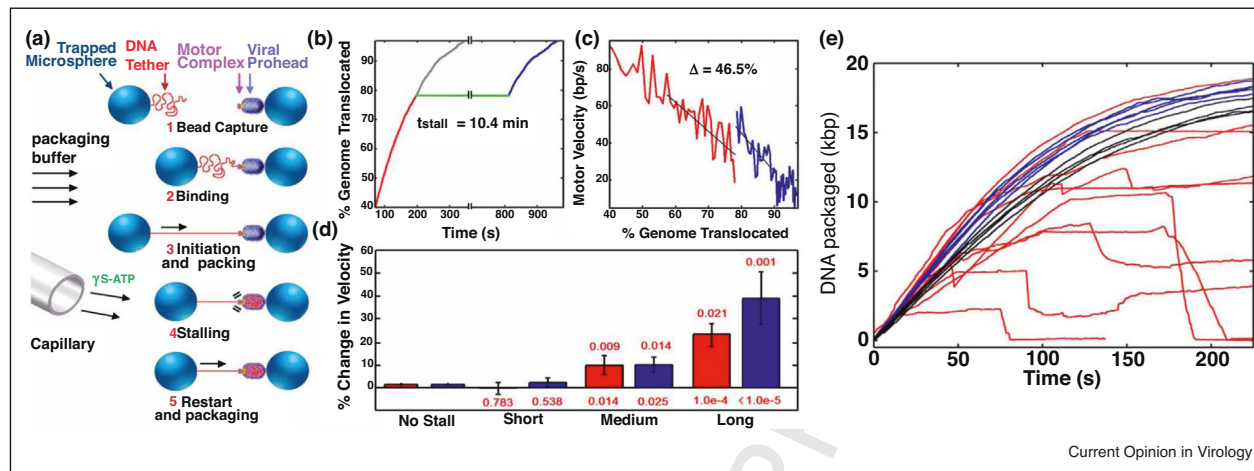
166 The first was an experiment where DNA packaging was
 167 initiated in the laser tweezers and then halted by the
 168 introduction of a nucleotide analogue, gamma-S-ATP,
 169 into the motor causing it to stall [17*]. After a range of
 170 times, the analogue was cleared and the velocity after the
 171 stall was measured and compared to the pre-stall mea-
 172 surement (Figure 4). What was predicted was that, if the
 173 DNA relaxes inside the head after packaging, then the

174 internal resistive force would decrease and velocity of
 175 translocation would increase relative to the speed just
 176 before the stall. This hypothesis was indeed supported,
 177 but the time-scale of relaxation observed was unexpect-
 178 edly long. In most simulations, the rate of DNA relaxation
 179 is considered to be so fast that it is nearly irrelevant on the
 180 timescale of the viral DNA packaging process. The
 181 dissipation experiments from the Smith lab suggest that
 182 the time scale of relaxation for DNA under confinement
 183 on the order of minutes, over five orders of magnitude
 184 slower than used in simulations [12*,18–20]. Arguably,
 185 DNA compacted to the high density seen in virus
 186 particles may in fact never completed reach an energy
 187 minimum, and is retained inside the head in a somewhat
 188 glassy state.

189 The second series of experiments from the Smith lab
 190 revealed another perspective on the issue. It is well under-
 191 stood that electrostatic screening of DNA charge reduces
 192 the repulsive force of charged phosphate backbones that
 193 are being forced together during packaging [21,22]. This
 194 was highlighted by a series of experiments where cations
 195 were varied in the phi29 packaging system and the force
 196 required for compaction showed a relative decrease when
 197 charge screening is high, that is in the presence of divalent
 198 magnesium, compared to less effective screening condi-
 199 tions, that is in the presence of monovalent sodium [23]. By
 200 extension, inclusion of more potent screening agents, such
 201 as cobalt hexamine or spermine, further reduced the force
 202 required to achieve high DNA density during filling
 203 [23,24*]. In experiments designed to test the limits of this
 204 phenomenon (Figure 4), higher levels of spermine were
 205 evaluated, but with an unexpected result: once spermine
 206 levels were increased to the point where the DNA could
 207 experience spontaneous condensation, rather than reliev-
 208 ing the resistive force of charge repulsion in the virus head,

4 Virus structure and expression

Figure 4



Current Opinion in Virology

Long relaxation time-scale and jamming during DNA packaging. (a) Experimental design, where packaging is initiated *in situ* by bringing prohead motor complexes in close contact with tethered DNA (steps 1 and 2). After packaging is initiated and the rate of DNA translocation determined (step 3), the phi29 motor is reversibly stalled (step 4) and, after a prescribed time, restarted to determine if the rate of packaging has increased relative to the rate before the stall (step 5). (b) Measurement of DNA tether length over time taken before (red trace) and after (blue trace) the analogue induced stall (green trace). When the post-stall trace is transposed to the point of the stall (grey trace), the inflection in the trace reveals the increase in packaging velocity after the stall. (c) An example trace where the motor velocity before (red trace) and after (blue trace) the stall are plotted relative to the amount of head filling, showing that the motor increased in velocity by 46.5% due to the stall. (d) The length of the stall time corresponds to increase in packaging rate, for both packaging velocity (red) and motor velocity (blue; edited for motor pauses/slips), indicative of a time-dependent process of DNA relaxation during the stall. (e) Jamming appears with the addition of spermine as a DNA condensing agent can be seen when observing packaging over time. At low concentrations of spermine, packaging rate increases compared to controls (blue versus black traces). Higher concentrations of spermine cause abrupt decelerations and translocation failures (red traces). Reprinted from Berndsen *et al.* [17^{**}] (a-d), and from Keller *et al.* [24^{**}] with permission from Elsevier (e).

209 stalling events appeared [24^{**}]. This ‘jamming’ phenomena, interpreted as the result of a bolus of static DNA
210 occluding the entrance of the head, is reminiscent of the
211 broader jamming behavior seen in macroscopic systems
212 such as particle flow in piping systems. In hindsight, this
213 observation is easy to rationalize, but revealed that some
214 repulsion of the DNA inside the virus particle is required to
215 prevent a terminal relaxation event, a final energy
216 minimum, that occurs with condensation rather than
217 compaction.

218 What emerges is a model whereby the complex physical
219 behavior of DNA places limits on packaging motor operation.
220 It would seem preferable that, during virus
221 assembly, the progression through the series of events
222 required to produce virions be as swift as possible.
223 However, the now apparent long time-scale of DNA relaxation
224 during confinement requires that the DNA packaging
225 event is throttled such that the packaged DNA is pro-
226 vided sufficient time to relax, thus preventing jamming.

227 Extending the model

228 These inferences are further supported by experiments
229 on other dsDNA phage systems. The larger phages, rather
230 than packaging a unit-length genome found in phi29,
231 package DNA retrieved from long concatamers [1[•],25]:

232 multiple genome lengths are linked as a result of a more
233 complex DNA replication strategy employed by these
234 phages. Therefore, during packaging, the amount of
235 DNA packaged is determined, in part, by the capacity
236 of the head. In these phages, packaging is ‘terminated’
237 but the endonuclease action of the packaging ATPase in a
238 sequence-dependent (ex. lambda) or sequence-
239 independent (ex. T4) manner (hence the term ‘terminase’)
240 is applied to packaging machinery of these systems). It
241 has been known for some time that such a head-full
242 packaging mechanism relies on sensing of the amount
243 of DNA in the capsid, ensuring that a chromosome of
244 sufficient length to code for the entire genome is pack-
245 aged. To this end, much effort has focused on the portal
246 connector that is embedded in the head shell through
247 which the DNA passes. Since the packaged DNA abuts
248 the portal, and can, therefore, directly register the increasing
249 pressure exerted by the DNA as the head fills, it may
250 act as a pressure switch that allosterically signals the
251 motor to slow [26[•],27,28]; it has been shown that muta-
252 tions in the portal of phages P22 and SPP1 can alter the
253 spatial timing of the termination event, since these
254 mutants package shorter chromosomes than wild type.

255 Measurement of packaging velocity in the coliphage
256 lambda [29] and T4 [30] systems showed that these

258 phages packaged DNA significantly faster than phi29.
 259 Phages lambda and T4, whose DNA are $\sim 2.5 \times$ and $8 \times$
 260 the length of phi29's, respectively, package DNA faster
 261 than phi29 by roughly the same scale. The result is that
 262 packaging for all of these phages takes ~ 3 min *in vitro*,
 263 even though they range in chromosome size from less
 264 than 20 kb to over 160 kb. Hence, it is tempting to
 265 speculate that the time scale of packaging is determined
 266 not by the resistive force and work involved, but rather
 267 the time required for the DNA to relax upon and during
 268 confinement; this appears to be independent of the length
 269 of the viral chromosome since the length of the DNA
 270 scales proportionally with the size of the capsid
 271 receptacle. Although not yet measured experimentally,
 272 it is possible that DNA translocation during early filling in
 273 T4, which occurs at a velocity similar to the actual
 274 translocation rate measured in phi29, that is 1000 bp/
 275 sec, can operate without the need for the throttling
 276 behavior seen in phi29 that appears manifest in the
 277 relatively long and regulated dwell phase of the packag-
 278 ing mechanism; phage lambda would be predicted to fall
 279 between phi29 and T4, with a similar translocation
 280 velocity and intermediate dwell time. It also remains to
 281 be seen whether the phages with larger genomes such as
 282 lambda and T4 reduce their DNA translocation rate at
 283 high filling via an allosteric mechanism that reduces the
 284 rate of nucleotide cycling seen in phi29. As well as giving
 285 the DNA enough time to relax inside the head shell, this
 286 regulatory mechanism, a 'head-filling sensor', may play a
 287 role in the critical termination event not found in phi29. It
 288 remains to be determined whether and how these events
 289 are related, or whether the sensing function in phi29, with
 290 its unit length chromosome, has lost the signaling for
 291 filling that determines chromosome length and retained
 292 the throttling function or acquired a throttling function by
 293 other means.

Conclusion

294 Taken together, this series of experiments and observa-
 295 tions reveal a complex physics at the submicroscopic level
 296 that DNA viruses experience, and have thus adapted to in
 297 order to produce infectious virus particles that can deliver
 298 DNA from cell to cell. Although speed would generally be
 299 considered an asset in terms of completing an assembly
 300 reaction to produce infectious virus during the short time
 301 scale of infection, the physical behavior of the DNA
 302 demands patience. That such a fundamental observation
 303 of the time-scales of DNA relaxation be revealed by
 304 observing a biological system is compelling.

Funding

305 **Q5** This work was supported by the National Institutes of
 306 Health (R01GM122979, R01GM071552 and
 307 R56AI127809) and the National Science Foundation
 308 (MCB 1715293).

References and recommended reading

Papers of particular interest, published within the period of review,
 have been highlighted as:

- of special interest
- of outstanding interest

1. Rao VB, Feiss M: **Mechanisms of DNA packaging by large double-stranded DNA viruses.** *Annu Rev Virol* 2015, **2**:351-378. 311
 An excellent introduction to the field of dsDNA viral packaging. 312
2. Speir JA, Johnson JE: **Nucleic acid packaging in viruses.** *Curr Opin Struct Biol* 2012, **22**:65-71. 313
3. Garcia HG, Grayson P, Han L, Inamdar M, Kondev J, Nelson PC, Phillips R, Widom J, Wiggins PA: **Biological consequences of tightly bent DNA: the other life of a macromolecular celebrity.** *Biopolymers* 2007, **85**:115-130. 318
4. Knobler CM, Gelbart WM: **Physical chemistry of DNA viruses.** *Annu Rev Phys Chem* 2009, **60**:367-383. 319
5. Chemla YR, Smith DE: **Single-molecule studies of viral DNA packaging.** *Adv Exp Med Biol* 2012, **726**. 320
6. Grimes S, Jardine PJ, Anderson D: **Bacteriophage φ 29 DNA packaging.** *Adv Virus Res* 2002, **58**:255-280. 321
7. Iyer LM, Makarova KS, Koonin EV, Aravind L: **Comparative genomics of the FtsK-Hera superfamily of pumping ATPases: implications for the origins of chromosome segregation, cell division and viral capsid packaging.** *Nucleic Acids Res* 2004, **32**:5260-5279. 322
8. Mao H, Saha M, Reyes-Aldrete E, Sherman M, Woodson M, Atz R, Grimes S, Jardine P, Morais M: **Structural and molecular basis for coordination in a viral DNA packaging motor.** *Cell Rep* 2016, **14**:2017-2029. 323
9. Morais MC, Koti JS, Bowman VD, Reyes-Aldrete E, Anderson DL, Rossmann MG: **Defining molecular and domain boundaries in the bacteriophage φ 29 DNA packaging motor.** *Structure* 2008, **16**:1267-1274. 324
10. Ding F, Lu C, Zhao W, Rajashankar KR, Anderson DL, Jardine PJ, Grimes S, Ke A: **Structure and assembly of the essential RNA ring component of a viral DNA packaging motor.** *Proc Natl Acad Sci U S A* 2011, **108**:7357-7362. 325
11. Smith DE, Bustamante C, Tans SJ, Smith SB, Grimes S, Anderson DL: **The bacteriophage straight phi29 portal motor can package DNA against a large internal force.** *Nature* 2001, **413**:748-752. 326
- The first single-molecule laser tweezers study of viral DNA packaging. 327
12. Kindt J, Tzilil S, Ben-Shaul A, Gelbart WM: **DNA packaging and ejection forces in bacteriophage.** *Proc Natl Acad Sci U S A* 2001, **98**:13671-13674. 328
- Early comprehensive modelling study of DNA confinement during packaging. 329
13. Chemla YR, Aathavan K, Michaelis J, Grimes S, Jardine PJ, Anderson DL, Bustamante C: **Mechanism of force generation of a viral DNA packaging motor.** *Cell* 2005, **122**:683-692. 330
14. Moffitt JR, Chemla YR, Aathavan K, Grimes S, Jardine PJ, Anderson DL, Bustamante C: **Intersubunit coordination in a homomeric ring ATPase.** *Nature* 2009, **457**:446-450. 331
15. Chistol G, Liu S, Hetherington CL, Moffitt JR, Grimes S, Jardine PJ, Bustamante C: **High degree of coordination and division of labor among subunits in a homomeric ring ATPase.** *Cell* 2012, **151**:1017-1028. 332
16. Liu S, Chistol G, Hetherington CL, Tafoya S, Aathavan K, Schnitzbauer J, Grimes S, Jardine PJ, Bustamante C: **A viral packaging motor varies its DNA rotation and step size to preserve subunit coordination as the capsid fills.** *Cell* 2014, **157**:702-713. 333
- Extensive single-molecule studies of viral packaging motor coordination and DNA movement across the head-filling regime. 334
17. Berndsen ZT, Keller N, Grimes S, Jardine PJ, Smith DE: **Nonequilibrium dynamics and ultraslow relaxation of confined** 335

6 Virus structure and expression

361 **DNA during viral packaging.** *Proc Natl Acad Sci U S A* 2014,
362 111:8345–8350. 384

363 Single-molecule laser tweezers study of relaxation of DNA inside the viral
364 capsid revealing the time-scale of DNA relaxation is orders of magnitude
365 slower than assumed. 385

366 18. Forrey C, Muthukumar M: **Langevin dynamics simulations of**
367 **genome packing in bacteriophage.** *Biophys J* 2006, 91:25–41. 386

368 19. Petrov AS, Harvey SC: **Structural and thermodynamic**
369 **principles of viral packaging.** *Structure* 2007, 15:21–27. 387

370 20. Ali I, Marenduzzo D, Yeomans JM: **Polymer packaging and**
371 **ejection in viral capsids: shape matters.** *Phys Rev Lett* 2006,
372 96:208102. 388

373 21. Bloomfield VA: **DNA condensation by multivalent cations.**
374 *Biopolymers* 1997, 44:269–282. 389

375 22. Rau DC, Parsegian VA: **Direct measurement of the**
376 **intermolecular forces between counterion-condensed DNA**
377 **double helices. Evidence for long range attractive hydration**
378 **forces.** *Biophys J* 1992, 61:246–259. 390

379 23. Fuller DN, Rickgauer JP, Jardine PJ, Grimes S, Anderson DL,
380 Smith DE: **Ionic effects on viral DNA packaging and portal**
381 **motor function in bacteriophage φ 29.** *Proc Natl Acad Sci U S A*
382 2007, 104:11245–11250. 391

383 24. Keller N, Grimes S, Jardine PJ, Smith DE: **Single DNA molecule**
384 **jamming and history-dependent dynamics during motor-**
385 **driven viral packaging.** *Nat Phys* 2016, 12:757–761. 392

386 Single-molecule study of jamming behavior during packaging in the
387 presence of DNA-condensing ions that provide evidence that DNA
388 charge repulsion is not simply a barrier but also permits DNA rearrange-
389 ment during packaging. 393

390 25. Feiss M, Rao VB: **The bacteriophage DNA packaging machine.**
391 *Adv Exp Med Biol* 2012, 726:489–509. 394

392 26. Lokareddy RK, Sankhala RS, Roy A, Afonine PV, Motwani T,
393 Teschke CM, Parent KN, Cingolani G: **Portal protein functions**
394 **akin to a DNA-sensor that couples genome-packaging to**
395 **icosahedral capsid maturation.** *Nat Commun* 2017, 8:14310. 395

396 Recent structural work examining the role of the dsDNA viral portal in
397 packaging. 396

398 27. Tavares P, Zinn-Justin S, Orlova EV: **Genome gating in tailed**
399 **bacteriophage capsids.** *Adv Exp Med Biol* 2012, 726:585–600. 399

400 28. Oliveira L, Tavares P, Alonso JC: **Headful DNA packaging:**
401 **bacteriophage SPP1 as a model system.** *Virus Res* 2013,
402 173:247–259. 400

403 29. Fuller DN, Raymer DM, Rickgauer JP, Robertson RM,
404 Catalano CE, Anderson DL, Grimes S, Smith DE: **Measurements**
405 **of single DNA molecule packaging dynamics in bacteriophage**
406 **λ reveal high forces, high motor processivity, and capsid**
407 **transformations.** *J Mol Biol* 2007, 373:1113–1122. 401

408 30. Fuller DN, Raymer DM, Kottadiel VI, Rao VB, Smith DE: **Single**
409 **phage T4 DNA packaging motors exhibit large force**
410 **generation, high velocity, and dynamic variability.** *Proc Natl*
411 *Acad Sci U S A* 2007, 104:16868–16873. 402